



Integrating geoelectrical and geological techniques in GIS-based DRASTIC model of groundwater vulnerability potential in the raffia city of Ikot Ekpene and its environs, southern Nigeria

A. M. Ekanem¹ · E. O. Ikpe² · N. J. George¹ · J. E. Thomas¹

Received: 3 April 2022 / Accepted: 13 June 2022 / Published online: 13 July 2022

© The Author(s), under exclusive licence to Iranian Society of Environmentalists (IRSEN) and Science and Research Branch, Islamic Azad University 2022

Abstract

Groundwater contamination is a major concern in the raffia city of Ikot Ekpene as a result of increasing domestic and industrial wastes occasioned by increasing human population coupled with other commercial activities in the area. This study, therefore, aims at assessing groundwater vulnerability in the raffia city of Ikot Ekpene and its environs in southern Nigeria using integrated geoelectrical and geological techniques in the GIS-based DRASTIC model. Twenty vertical electrical soundings (VES) were made in the area with the use of the Schlumberger array. The results of the VES data interpretation as constrained by the geological borehole data indicate that the area comprises 3–4 geoelectric layers. The lithological sequence in the area varies from fine to coarse sand and gravelly sands with pockets of clay intercalations at some locations. The third geoelectric layer, which occurs at a depth of 9.0–86.6 m, is the major exploitable aquifer in the area. Seven environmental parameters (depth to the water table, net recharge, aquifer media, topography, impact of vadose zone and hydraulic conductivity) were used for the vulnerability assessment in the DRASTIC model. In terms of groundwater vulnerability ratings (GVR), the result of the assessment shows that 75% of the study area falls under high, 20% falls under moderate while the remaining 5% falls under low ratings respectively. On the whole, 95% of the study area is characterized by moderate/high GVR possibly due to the general lower slope terrain in the area, which comprises mostly high permeable geomaterials in the overlying water table layers. The high groundwater vulnerability zone has been demarcated in the vulnerability map generated and this could be very helpful in effective groundwater management and abstraction in the area.

Keywords DRASTIC · GIS · Aquifer media · Permeability · Groundwater vulnerability · Topography

Introduction

Groundwater is increasingly desirable as a source of potable water for the world's teeming population, partly because of its availability and secondly, due to its relatively better quality when compared with surface water sources such as streams, lakes, rivers etc. Groundwater is stored underground in rock units known as aquifers, which are not visible to the human eyes. These aquifers can be susceptible to pollution or contamination from either natural or anthropogenic

sources such as wastes from poor waste disposal, inappropriate sewerage systems, mining activities, intensive agriculture, industrialization and urbanization (Ekanem, 2022; Ekanem et al., 2022; Kumar & Krishna, 2020; Machiwal et al., 2018). These activities cause groundwater to be contaminated and therefore unfit for human use. As a matter of fact, groundwater contamination has become an issue of global concern in recent times as a result of its enormous impacts on human health as well as ecological services (Ekanem, 2022; George, 2021; Ikpe et al., 2022; Li et al., 2021). Consequently, groundwater vulnerability assessment has become an efficient tool to delineate areas that are prone to contamination, all in an effort to formulate effective groundwater management and groundwater protection schemes (Ekanem, 2022; Ikpe et al., 2022; Kumar & Krishna, 2020).

Groundwater vulnerability potential refers to the degree of protection offered by the natural environment against the spread of contaminants in groundwater. The geology of an

✉ A. M. Ekanem
anny4mart@yahoo.com; aniekanekem@aksu.edu.ng

¹ Department of Physics, Geophysics Research Group (GRG), Akwa Ibom State University, Mkpato Enin, Nigeria

² Department of Science Technology, Akwa Ibom State Polytechnic, Ikot Osurua, Ikot Ekpene, Nigeria

area controls the amount of time taken by surface contaminated water for instance from rainwater to percolate through the soil to the water table (Ekanem, 2020; George, 2021). Surface contaminants or pollutants can infiltrate to contaminate groundwater depending on the nature of the geomaterials above the water table. Vulnerability in this case refers to how easy it is for surface or near surface contaminants to infiltrate to underground hydrogeological units to pollute or contaminate groundwater (Foster et al., 2013; Harter & Walker, 2001). The degree of contamination depends largely on the time taken by the contaminants to reach the water table (Maxe & Johansson, 1998), which is of course a function of the depth of the water table, characteristics of the vadose zone, net recharge and the geochemical properties of the contaminants (Abu-Bakr, 2020; Kumar & Krishna, 2020). Shallow aquifers are thus more susceptible to contaminants than deeper ones. Groundwater vulnerability may be grouped into intrinsic (natural) and specific (integrated) vulnerabilities respectively (NRC, 1993; Vrba and Zoporozec, 1994). Intrinsic or natural vulnerability, which takes into consideration the geological, hydrological and hydrogeological features of an area, refers to the ease with which surface originated contaminants regardless of their nature can permeate into the water table and diffuse in groundwater (Vrba and Zoporozec, 1994). Specific vulnerability on the other hand refers to groundwater contamination caused by a particular contaminant or group of contaminants and is determined by the properties of the contaminants, taking into consideration the time and intensity of the impact of the contaminant and the interaction between the intrinsic vulnerability components and the contaminant in question (Doerfliger et al., 1999; Gogu & Dassargues, 2000a).

Several methods are available for carrying out groundwater vulnerability assessment. These methods include the DRASTIC method (Aller et al., 1987), GOD method (Foster, 1987), AVI method (Van Stempvoort et al., 1992), the SINTACS method (Civita, 1990) and the SI method (Boufekane & Saighi, 2013). Among these methods, the DRASTIC method is the most popular because it is very easy to use; the required data are very easy to get and it gives a lucid explanation of groundwater vulnerability (Awawdeh & Jaradat, 2010; Neh et al., 2014; Awawdeh et al., 2015; Barbulescu, 2020). This method utilizes seven parameters for vulnerability assessment (Aller et al., 1987). The parameters are depth to groundwater (D), net recharge (R), aquifer media (A), soil media (S), topography (T), impact of vadose zone (I) and aquifer hydraulic conductivity (C), forming the acronym 'DRASTIC'. These input parameters, which are readily available help to minimize the effects of errors of the individual parameters on the final results and thus make the model a great tool for groundwater vulnerability assessment. The major drawback of the DRASTIC model is the subjectivity in the assignment of weights and ratings to the

different parameter components of the model (Gogu & Dassargues, 2000b; Chitsazan and Akhtari, 2008). All the same, the model has been successfully used to assess groundwater vulnerability in many parts of the world (Abdullahi, 2009; Abu-bakr, 2020; Amiri et al., 2020; Awawdeh & Jaradat, 2010; Awawdeh et al., 2015; Barbulescu, 2020; George, 2021; Kumar & Krishna, 2020; Shirazi et al., 2013; Venkatesan et al., 2019).

In this study, the DRASTIC model was adopted to assess the groundwater vulnerability of the raffia city of Ikot Ekpene and its environs in southern Nigeria. All the input parameters in the DRASTIC model were obtained from the VES data interpretation results apart from topography, which was determined from the ASTER digital elevation model (DEM) through the use of ArcGIS 10.5. The VES technique has proven to be an important tool for the investigation of electrical resistivity variation pattern of the subsurface and constitutes a rapid and cost effective means of imaging subsurface aquifers (Ekanem et al., 2020; George, 2021; Ikpe et al., 2022; Udoh et al., 2015). Unlike the conventional well drilling, the VES technique is less expensive and environmentally friendly since it only requires surface measurements without the need for actual drilling of boreholes (Ekanem et al., 2020; George et al., 2018; Udoh et al., 2015). Ikot Ekpene, with inadequate surface water bodies, has experienced water scarcity problems over the years due to rapid population increase and urbanization (George et al., 2016a, 2017; Ikpe et al., 2022). There has been a continuous heavy dependence on groundwater georesource to meet the increasing water needs of the people of Ikot Ekpene municipality and its environs. The resultant effect of this increasing human population coupled with other commercial activities in the area is a corresponding increase in both domestic and industrial wastes in the area. Indiscriminate waste disposal has become a major challenge in Ikot Ekpene municipality as heaps of solid wastes comprising domestic wastes, vegetable wastes, waste papers, scrap metals, cans containing different chemicals, plastic containers, old rags, vehicle tyres, scalpels and human wastes continue to litter the streets in the area (Ikpe et al., 2022; Umoh & Etim, 2013). During rainfall, some of these hazardous wastes find their ways into the hydrogeological units in the area to cause groundwater contamination, which pose serious challenges to human health as well as other ecological services. George et al. (2014) integrated geophysical, geochemical and hydrogeological measurements to assess the effect of leachates on groundwater quality around the old dumpsite of this study area. Their results showed that the effect of leachates was more pronounced in the identified groundwater repositories in close proximity to the dumpsite than farther away from it. Recently, Ikpe et al. (2022) used the VES and electrical resistivity tomography (ERT) techniques to appraise the protectivity of hydrogeological units in this study area. The results of

their appraisal revealed that 75% of the study area has poor/weak protectivity rating, 20% has moderate while only 5% has good protectivity ratings respectively. The implication of these findings is that the topmost cover layers of the study area may be extremely vulnerable to surface or near surface contaminants. This study was therefore necessary to map out the high vulnerability zones in the area to help in the formulation of an efficient groundwater development and exploration scheme as well as proper waste disposal scheme in the area by the appropriate agencies respectively.

Description of the study area and its brief geology

This study was conducted in the raffia city of Ikot Ekpene and its environs in southern Nigeria (Fig. 1). The area lies between latitudes 5.072° – 5.140° N and longitudes 7.390° – 7.458° E respectively and covers an area of about 119 km^2 . The maximum elevation above mean sea level in the area is 102 m in the northern part while the minimum elevation is 54 m in the southern part. The city is accessible by a network of roads and is one of the commercial business hubs in Akwa Ibom state, southern Nigeria. The area is drained by the inland coastal water and the vegetation is of the rain forest type. Average annual rainfall in the area is about 2007.9 mm (Isaiah et al., 2021).

Climatically, the raffia city of Ikot Ekpene is situated in a region with a humid tropical climate and is characterized

by two seasons. These seasons are the dry season, which spans from November to April and the rainy or wet season (spanning from March to October) (). The prevailing wind pattern in the area during the dry season is the Harmattan winds from the north while the Monsoon winds from the Atlantic Ocean prevail during the wet season (Vrbka et al., 1999). Annual temperatures in the study area range from 20°C in the wet or rainy season to about 35°C in the dry season (Ekanem, 2020; George et al., 2017, 2021).

In terms of geology, the raffia city of Ikot Ekpene is situated in the Niger Delta province sitting directly on the Gulf of Guinea on the Atlantic Ocean in Southern Nigeria. The province is divided into three main stratigraphic units, which are the Benin Formation, the Agbada Formation and the Akata Formation at the base of the Delta (Obaje, 2009; Short & Stauble, 1967; Stacher, 1995) as illustrated in the schematic diagram of Fig. 2. The Benin Formation is the youngest and topmost part of the Niger Delta and comprises Coastal Plain sands (CPS) ranging in sizes from fine to coarse and gravels (Mbipom et al., 1996; Short & Stauble, 1967). Groundwater abstraction in the raffia city of Ikot Ekpene is done in the Coastal Plains of the Benin Formation, which is characterized by pockets of intercalations of clay, silts and sandstones at many locations (Reijers et al. 1987). A multi-aquifer system is built up by the alternating sand and clay sequence at some locations in the study area (Edet & Okereke, 2002; Esu et al., 1999).

Fig. 1 Map of a Nigeria showing Akwa Ibom State in southern Nigeria. **b** Akwa Ibom State showing the study area, **c** study area showing its geology and sounding stations

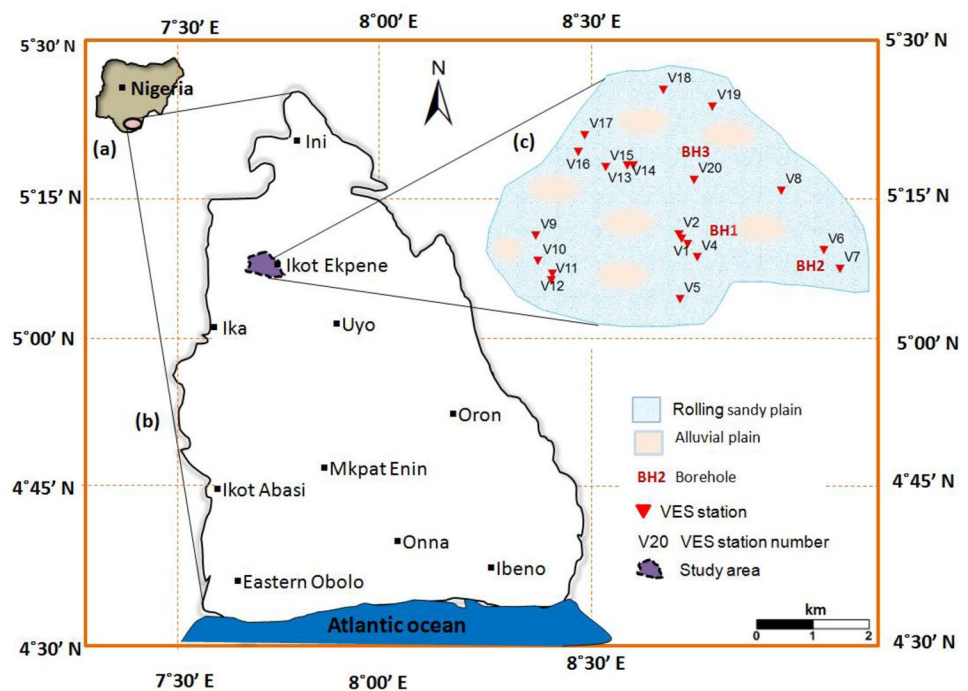
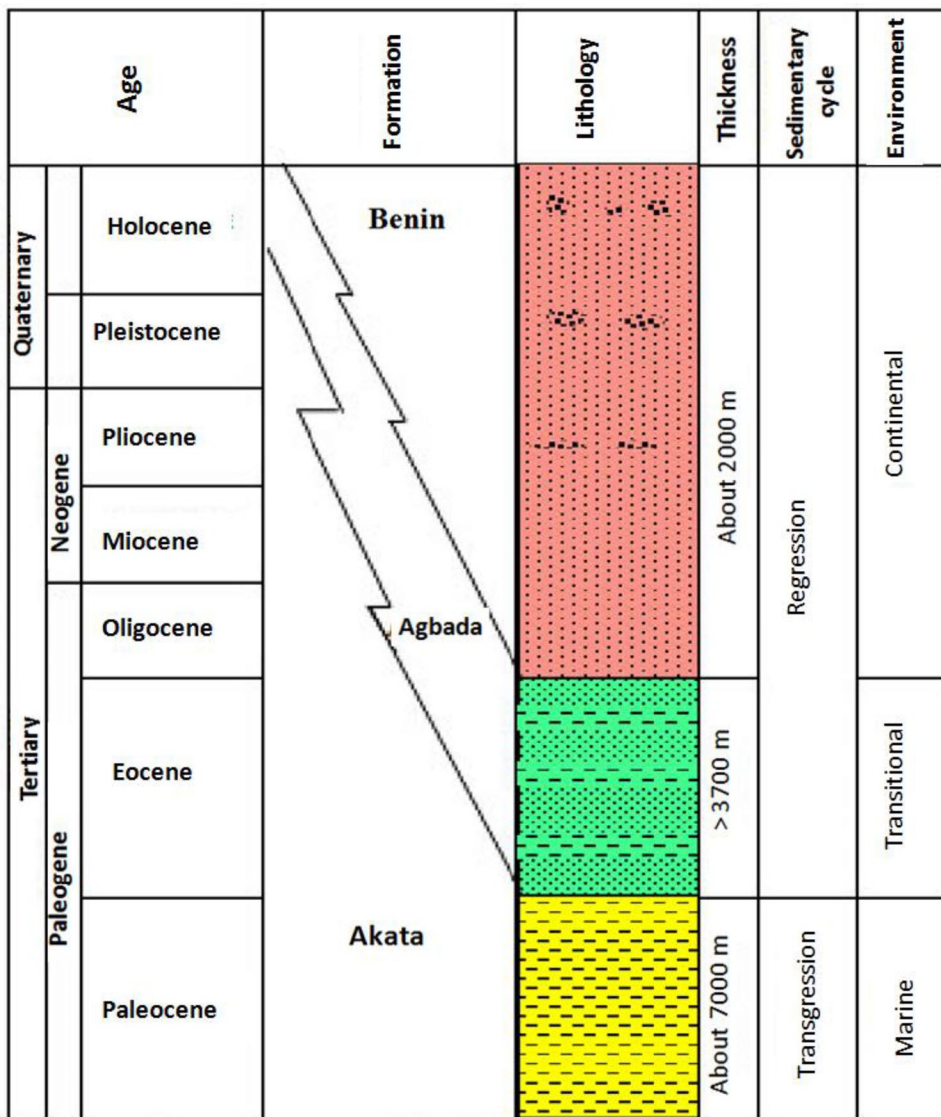


Fig. 2 A schematic diagram showing the general Stratigraphy of the Niger Delta, where the study area is located (adapted from Obaje, 2009)



Materials and methods

Two sets of data were utilized in this study in conjunction with the GIS-based DRASTIC model to assess groundwater vulnerability in the raffia city of Ikot Ekpene and its environs. These datasets are the geophysical data acquired using the electrical resistivity technique and the borehole geological data. The electrical resistivity technique involved the use of the Schlumberger electrode configuration to carry out vertical electrical soundings (VES) in the study area. The resistivity data acquired were interpreted using the WINRESIST software program to get the first order geoelectric properties of the layers penetrated by electric current. These properties are resistivity, thickness and depth. The borehole lithological logs from drilled boreholes in the study area were used as controls in the identification of the various lithological and hydrogeological units from the interpreted resistivity data.

VES data acquisition, analysis and interpretation

The IGIS signal enhancement resistivity meter SSP-MP-ATS and its accessories was used to carry out a one-dimensional (1D) electrical resistivity sounding in different locations in the raffia city of Ikot Ekpene and its environs as shown in Fig. 1. The Schlumberger electrode configuration was adopted in the field survey as in Bello et al (2010), Udoh et al. (2015), George et al., (2014, 2017, 2018, 2021), Thomas et al. (2020), Ekanem et al. (2021) etc.. This configuration comprises two current electrodes A and B, used to inject a well-defined electric current into the subsurface and two potential electrodes M and N to detect the resulting potential difference respectively. The four electrodes were planted on the earth surface on a straight line. The resistivity meter gave the apparent resistance of the earth layers as its LCD displayed output in ohms (Ω). The current electrode

separation AB was gradually increased about the centre of the sounding for deeper current penetration while the potential electrode separation MN was also occasionally increased (Ekanem et al., 2020; George et al., 2018, 2020; Thomas et al., 2020). Maximum AB in this study was 400 m while maximum MN was 20 m. In all the sounding stations occupied, it was ensured that the electrode spacing was such that $AB/2 \geq 5 MN/2$ in line with the potential gradient assumption (Dobrin & Savit, 1988). Three of the soundings were made close to three water boreholes in the area as shown in Fig. 1 where the borehole lithological logs were used to constrain the VES data interpretation during the computer modelling stage. The logs were used to constrain the initial layer thicknesses and depths during the modelling stage and also aided in the delineation of the various lithological and hydrogeological units in the area from the final modelling curves.

First, the raw apparent resistance (R_a) measured in the field was converted into apparent resistivity ρ_a by the use of Eq. (1):

$$\rho_a = \pi \times \left\{ \frac{\left(\frac{AB}{2}\right)^2 - \left(\frac{MN}{2}\right)^2}{MN} \right\} \times R_a \quad (1)$$

The values of the apparent resistivity calculated for each of the VES locations were then plotted against half of the current electrode separations (AB/2) on a bi-logarithmic scale to produce the VES sounding curves. The curves were manually smoothed to remove any spurious signature, which will likely lead to high root mean square errors (RMSE) during the computer-aided stage of the data interpretation (Chakravarthi et al., 2007; Ekanem, 2021, 2022; George et al., 2017). Any variations in the resulting smoothed curves were strictly attributed to the vertical resistivity distribution in the subsurface. Partial curve matching was done on the smoothed curves to generate the initial thicknesses and resistivities of the layers (Zohdy et al., 1974). These initial parameters were then used as inputs in the computer-aided interpretation carried out using the WIN-RESIST computer software program with the borehole lithological logs as controls. The computer software calculates a theoretical model using the initial layer parameters and establishes a match with the field data to give the final VES curves. The goodness of the match is provided by the root mean square errors. The final 1D resistivity model curves allow the true thickness, resistivity and depth of the various litho units to be determined. Samples of final VES curves and their correlations with the available lithological logs are shown in Fig. 3. The results of VES interpretations correlate fairly well with the borehole lithological logs, even though the inferred depths of the layers are a bit at variance with the

depths from the logs. This is possible because there may not be a perfect coincidence of geologic section and geoelectric sections (Bello et al., 2010).

Drastic model for groundwater vulnerability assessment

DRASTIC is an acronym for Depth (D), Net recharge (R), aquifer media (A), soil media (S), topography (T), impact of the vadose zone (I) and hydraulic conductivity of the aquifer (C). These seven parameters are combined to have the DRASTIC model. DRASTIC model was developed by the US Environmental Protection Agency (Aller et al., 1987; US EPA, 1994) and is a widely used model for groundwater vulnerability assessment (Awawdeh & Jaradat, 2010; Barbulescu, 2020). Each of the seven parameters is assigned a weight (W), which ranges from 1 to 5 depending on its level of severity on groundwater vulnerability (Aller et al., 1987). The weight of 5 is assigned to the most severe parameters while 1 is assigned to the least severe ones. The weights of the parameters according to Aller et al. (1987) and Barres-Lallemend (1994) are summarized in Table 1. Again, each of the seven parameters is divided into classes, which are characterized as ranges. Each range is assigned a rating (r) from 1 to 10 as shown in Table 1. The rating 10 is attributed to the parameter with highest impact on groundwater vulnerability while 1 is assigned to the parameter with the least impact on groundwater vulnerability. The DRASTIC index is calculated by the use of Eq. (2) (Knox et al., 1993).

$$\begin{aligned} \text{DRASTIC Index} = & D_r D_w + R_r R_w + A_r A_w + S_r S_w \\ & + T_r T_w + I_r I_w + C_r C_w \end{aligned} \quad (2)$$

The index is used to rate the groundwater vulnerability according to the modified classification of Aller et al. (1987) and Amiri et al. (2020) given in Table 2. The higher the DRASTIC index, the more the groundwater vulnerability potential and vice versa.

Results and discussion

VES data interpretation results

The results of the VES data interpretation reveal 3 to 4 geoelectric layers with their corresponding resistivities, thicknesses and depths as summarized in Table 3. The lithology of the geoelectric layers was interpreted from the resistivity distribution pattern constrained by the geological borehole lithological data from the available boreholes in the area. The topmost layer (layer 1) was interpreted as the motley topsoil and has resistivity values ranging from 157.3 to

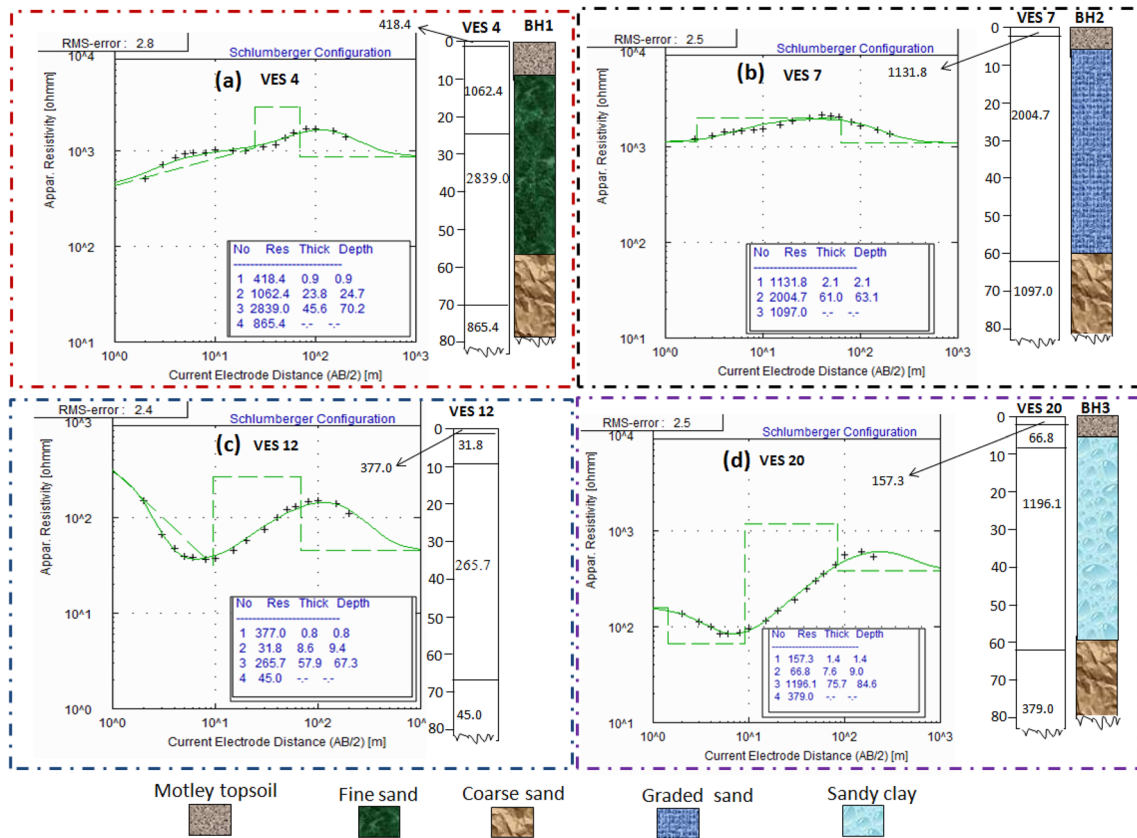


Fig. 3 Sample interpreted VES curves **a** VES 4—Utu Ikpe, **b** VES 7—Utu Uyo Road, **c** VES 12—AKWAPOLY, **d** VES 20 Library Avenue. The inserted legends show correlations of borehole lithological

logs with the VES results at VESs 4, 7 and 20. The results of VES interpretations correlate fairly well with the borehole lithological logs

1278.2 Ωm and thickness of 0.6 to 19.2 m. The high variability in the resistivity observed in this motley topsoil may be attributed to the false nature of the layer in addition to the ongoing bioturbating activities in the layer (Ekanem et al., 2021; George et al., 2016a). The motley topsoil is underlain by the second layer whose resistivity values vary between 31.8 to 2648.10 Ωm and thickness between 7.6 and 80.9 m. This layer was interpreted as sandy clay at some locations and fine/graded sands at some other locations. The high variability in the resistivity observed in this layer may again be the results of the variability in grain sizes of the geomaterials of the layer, which characterizes the Coastal Plain sands of the Niger Delta province (Ekanem, 2021; Mbipom et al., 1996). The third layer, which occurs at a depth of 9.0 to 86.6 m has a resistivity range of 214.4 to 2839.0 Ωm . Based on the resistivity variation pattern and information from the available borehole lithological logs in the area, this layer constitutes the major exploitable hydrogeological units (aquifers) in the study area. The layer was interpreted as fine/coarse sands/sandy clay at some locations and gravelly sands at other locations as constrained by the borehole lithological logs and hence exhibits a wide range of

resistivity variation as observed. The aquifer properties are summarized in Table 4. The aquifers are devoid of confining impermeable layers and are therefore generally unconfined. The fourth and of course the last geoelectric layer identified and interpreted as fine sands at some locations (VESs 1, 4, 5, 8, 18 and 20) and sandy clay at other locations (VESs 11, 12 and 17) has resistivity values ranging from 45.0 to 865.4 Ωm . The maximum current electrode separations of 400 m could not enable the injected current to penetrate to the bottom of this last layer and hence its thickness and depth could not be ascertained. These interpretations are similar to those of George et al. (2014) and Ikpe et al. (2022) in the study area. The factors, which might affect the resistivity results in this study, are density, shape, size, pore size and porosity, lithology, water content, clay content, and salinity.

Results of groundwater vulnerability assessment

Depth to water table the depth to the water table was estimated from the VES interpretation results and ranges from 9.0 to 86.6 m (Fig. 4a). The deeper the water table, the less vulnerable groundwater is to surface contaminants and vice

Table 1 Ranges, ratings and weight of DRASTIC factors (Aller et al., 1987; Barres-Lallemend, 1994)

Depth of water (m)	Aquifer media		Soil media		Topography		Impact of vadose zone		Hydraulic conductivity (m/s)					
	R	W	R	W	Interval	R	W	Interval	R	W				
<20	10	5	2	3	Thin or absent	10	2	0–5	10	1	Thin or absent	10	5	> 9.4 × 10 ⁻⁴
20–40	9		3		Gravel	10			10		Gravel	10		4.7 × 10 ⁻⁴ –9.4 × 10 ⁻⁴
40–60	7		4		Sand	9		5–15	9		Sand	9		32.9 × 10 ⁻⁵ –4.7 × 10 ⁻⁴
60–80	5		5		Laterite/peat	8		15–25	8		Laterite/peat	8		14.7 × 10 ⁻⁴ –32.9 × 10 ⁻⁵
80–100	3		6		Shrinking and/aggregated clay	7			7		Shrinking and/aggregated clay	7		4.7 × 10 ⁻⁵ –14.7 × 10 ⁻⁵
100–120	2				Limestone and Shale	6			6		Sandy Loam	6		
>120	1		6		Sequences	5		25–35	5		Loam	5		4.7 × 10 ⁻⁷ –4.7 × 10 ⁻⁵
			6		Massive Sandstone	4			4		Silty Loam	4		
			6		Massive Limestone	3		>35	3		Clay Loam	3		
			8		Sand and Gravel	2			2		Muck	2		
			9		Basalt	1			1		Nonshrinky and Nonaggregated clay	1		
			10		Karst Limestone									

Table 2 DRASTIC Index and Vulnerability Class (modified from Aller et al., 1987, Amiri et al., 2020)

DRASTIC Index (DI)	Vulnerability Class
1 – 100	Low
101 – 175	Moderate
176 – 200	High
> 200	Very high

versa (Amiri et al., 2020; George, 2021). The depth rating varies from 3 to 10 as shown in Fig. 4b. Majority of the study area is characterized by depth rating of greater than 5, which implies that the area is highly susceptible to groundwater pollution or contamination by surface contaminants. On the whole, the image map of Fig. 4 shows that pockets of highest groundwater vulnerability zones occur around Umuahia Road, Progress road, Ikpon road, Utu Ikpe community and Akwapoly.

Net recharge R this is the total amount of water from rainfall and other artificial sources that can percolate down to the water table. Net recharge constitutes the most important channel through which surface contaminants can enter into the aquifer to contaminate groundwater and is consequently positively linked with the vulnerability rating (Abdullahi, 2009; Shirazi et al., 2013). Rainfall constitutes the main source of groundwater recharge in the study area. In the absence of net recharge data in the area, the formulation of Piscopo (2001) was used to compute the net recharge value via the use of Eq. (3).

$$\text{Recharge value} = SF + RF + SPF \tag{3}$$

where *SF* is the slope factor, *RF* is the rainfall factor (mm) and *SPF* is the soil permeability factor. The average annual rainfall in the study area is about 2007.9 mm (Isaiah et al., 2021). The slope (in %) in the study area was obtained from the ASTER digital elevation model (DEM) via the use of ArcGIS 10.5. The DEM and slope obtained are given in Fig. 5a, b respectively. The soil hydraulic conductivity *K* was estimated in this study by the use of the empirical formula derived by Ekanem et al. (2020) for the area given by Eq. (4).

$$K = 139.12\rho_b^{-0.728} \tag{4}$$

where ρ_b is soil layer bulk resistivity. The soil permeability K_p was computed from the soil hydraulic conductivity via the use of Eq. (5).

$$K_p = \frac{K\mu_d}{\delta_w g} \tag{5}$$

where δ_w is water density (1000 kg/m³), *g* is acceleration due to gravity (9.8 m/s²) and μ_d is the dynamic viscosity of

Table 3 Summary of VES data interpretation results

VES No	Location	Longitude (Degrees)	Latitude (Degrees)	No. of Layers	Resistivity (Ωm)	Thickness (m)	Depth (m)	Lithology
1	Utu Ikpe 1	7.7038	5.1644	4	1190.2	2.6	2.6	Coarse sand
					248.6	8.5	11.1	Sandy clay
					1750.8	49.2	60.3	Gravelly sand
					418.7			Fine sand
2	Utu Ikpe 2	7.7031	5.1656	3	1278.2	5.6	5.6	Coarse sand
					639.4	56.7	62.3	Fine sand
					1621.6			Gravelly sand
3	Utu Ikpe 3	7.7053	5.1631	3	430.7	1.1	1.1	Fine sand
					2283.3	60.4	61.5	Gravelly sand
					851.2			Coarse sand
4	Utu Ikpe near Palace	7.7078	5.1598	4	418.4	0.9	0.9	Coarse sand
					1062.4	23.8	24.7	Coarse sand
					2839.0	45.6	70.3	Gravelly sand
					865.4			Fine sand
5	Abiakpo Edem Idim	7.7033	5.1491	4	1028.8	0.6	0.6	Coarse sand
					339.2	10.4	11.0	Sandy clay
					2129.4	54.0	65.0	Gravelly sand
					760.3			Fine sand
6	Ibiakpan Nto Akan	7.7400	5.1615	3	193.5	1.6	1.6	Sandy clay
					831.7	64.4	66.0	Fine sand
					1341.6			Coarse sand
7	Utu Uyo Road	7.7442	5.1568	3	1131.8	2.1	2.1	Coarse sand
					2004.7	61.0	63.1	Gravelly sand
					1097.0			Coarse sand
8	Ikpon Road	7.7292	5.1767	4	590.7	1.3	1.3	Fine sand
					149.2	11.1	12.4	Clay
					2478.6	61.4	73.8	Gravelly sand
					827.9			Fine sand
9	Abiakpo Ntak Inyang	7.6667	5.1652	3	487.8	2.1	2.1	Fine sand
					1021.5	53.5	55.6	Coarse sand
					2632.2			Gravelly sand
10	Akwa Poly 1	7.6672	5.1588	3	334.0	19.2	19.2	Sandy clay
					89.6	67.4	86.6	Clay
					214.4			Sandy clay
11	Akwa Poly 2	7.6706	5.1539	4	590.8	5.5	5.5	Fine sand
					72.1	16.7	22.2	Clay
					722.9	45.2	67.4	Fine sand
					83.3			Clay
12	Akwa Poly 3	7.6708	5.1556	4	377.0	0.8	0.8	Sandy clay
					31.8	8.6	9.4	Clay
					265.7	57.9	67.3	Sandy clay
					45.0			Clay
13	Ikot Ekpene Housing, Ifuho	7.6914	5.1832	3	441.5	3.6	3.6	Fine sand
					1848.3	63.4	67.0	Coarse sand
					2405.8			Gravelly sand
14	Ifuho 1	7.6900	5.1831	3	473.4	2.0	2.0	Fine sand
					79.4	52.3	54.3	Clay
					445.7			Fine sand

Table 3 (continued)

VES No	Location	Longitude (Degrees)	Latitude (Degrees)	No. of Layers	Resistivity (Ωm)	Thickness (m)	Depth (m)	Lithology
15	Ifuho2	7.6844	5.1827	3	170.7	1.7	1.7	Sandy clay
					925.1	68.1	69.8	Fine sand
					1959.4			Gravelly sand
16	Ibong Ikot Akan	7.6775	5.1866	3	228.5	6.1	6.1	Sandy clay
					2111.6	49.3	55.4	Gravelly sand
					434.5			Fine sand
17	Ibong Road	7.6792	5.1908	4	431.9	1.4	1.4	Fine sand
					40.6	14.6	16.0	Clay
					375.5	47.5	63.5	Fine sand
					75.6			Clay
18	Umuahia Road	7.6992	5.2024	4	224.4	2.1	2.1	Sandy clay
					59.1	8.4	10.5	Clay
					1264.5	59.9	70.4	Coarse sand
					324.9			Sandy clay
19	Ikono Road	7.7117	5.1981	3	207.4	4.5	4.5	Sandy clay
					2648.1	80.9	85.4	Gravelly sand
					1506.3			Coarse sand
20	Progress Road	7.7069	5.1794	4	157.3	1.4	1.4	Sandy clay
					66.8	7.6	9.0	Clay
					1196.1	75.7	84.7	Coarse sand
					379.0			Sandy clay

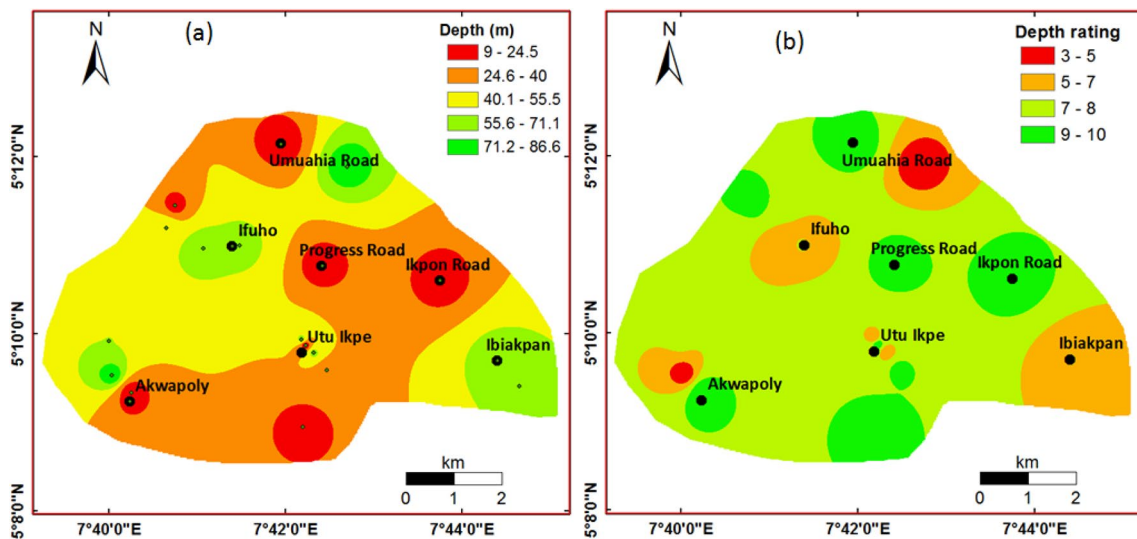
water, which was taken as 0.0014 kg/ms (Fetter, 1994). The computed values of K_p range between 1276.1 to 5865.2 mD. Accordingly, the slope, average annual rainfall and the soil permeability factors were rated according to the data given in Table 5. The rainfall factor was given a fixed value rating of 4 while the slope and soil permeability factors were rated from 1 to 4 respectively (Fig. 6). These ratings were stacked according to Eq. (3) to obtain the net recharge values for each of the sounding stations, which vary between 6 and 11 (Fig. 7a). Figure 7 indicates that relatively lower net recharge occurs in the southern part of the study area around Utu Ikpe community (Fig. 7a), which also corresponds to the area with lowest slope and soil permeability ratings shown in Fig. 6. The net recharge values were then reclassified based on the information in Table 5. The ratings of the net recharge values in the study area range from 3 to 10 as depicted in Fig. 7b. The least rating of 3–4 occurs in the southern part of the study area. Figure 8a, b respectively show the image maps of the DRASTIC depth and net recharge indices obtained from the multiplication of their respective ratings and weights. The depth index is least at pockets of locations in the northern part and near Akwapoly in the south western part of the study area while the net recharge index is least in the southern part and also near Akwapoly in Ikot Osurua community.

Aquifer media these refer to the geomaterials that constitute the aquifer. The permeability of the aquifer media, determined by the grains size of the aquifer materials (Ekanem et al., 2021) controls the attenuation of contaminants (Amiri et al., 2020; Venkatesan et al., 2019). Higher permeability aquifer geomaterials will lead to lower contaminants attenuation capacity and hence high vulnerability potential (Neh et al., 2015; Jaseela et al., 2016; Venkatesan et al., 2019; Amiri et al., 2020). In this study, the aquifer media were obtained from the VES data interpretation as constrained by the geological borehole lithological logs. The aquifer media comprise fine/coarse sands/sandy clay at some locations and gravelly sands at other locations. The sandy clay aquifer material was assigned a fixed rating of 3 while the sands and gravel were given a fixed rating of 8 according to Table 1. The weighting of aquifer media is 3 (Table 1). The image map of Fig. 9a shows the aquifer media index in the study area, which ranges from 9 to 24. The entire study area is characterised by high aquifer media index of greater than 13 except at a small spot around Akwapoly.

Soil media these refer to the topmost weathered part of the earth surface, where there are continuous bioturbating activities. Soil media greatly affect the quantity of rainfall recharge percolating down to the water table and the flow of contaminants (Jaseela et al., 2016; Amiri et al., 2020; George, 2021). Soils comprising gravel, sand and gravelly

Table 4 Summary of aquifer properties for the sounding locations

VES No	Location	Longitude (Degrees)	Latitude (Degrees)	Aquifer layer	Resistivity (Ω m)	Thickness (m)	Water table (m)	Lithology
1	Utu Ikpe 1	7.7038	5.1644	3	1750.8	49.2	11.1	Gravelly sand
2	Utu Ikpe 2	7.7031	5.1656	3	1621.6	–	62.3	Gravelly sand
3	Utu Ikpe 3	7.7053	5.1631	3	851.2	–	61.5	Gravelly sand
4	Utu Ikpe near Palace	7.7078	5.1598	3	2839.0	45.6	24.7	Gravelly sand
5	Abiakpo Edem Idim	7.7033	5.1491	3	2129.4	54.0	11.0	Gravelly sand
6	Ibiakpan Nto Akan	7.7400	5.1615	3	1341.6	–	66.0	Coarse sand
7	Utu Uyo Road	7.7442	5.1568	3	1097.0	–	63.1	Coarse sand
8	Ikpon Road	7.7292	5.1767	3	2478.6	61.4	12.4	Gravelly sand
9	Abiakpo Ntak Inyang	7.6667	5.1652	3	2632.2	–	55.6	Gravelly sand
10	Akwa Poly 1	7.6672	5.1588	3	214.4	–	86.6	Sandy clay
11	Akwa Poly 2	7.6706	5.1539	3	722.9	45.2	22.2	Fine sand
12	Akwa Poly 3	7.6708	5.1556	3	265.7	57.9	9.4	Sandy clay
13	Ikot Ekpene Housing, Ifuho	7.6914	5.1832	3	2405.8	–	67.0	Gravelly sand
14	Ifuho 1	7.6900	5.1831	3	445.7	–	54.3	Fine sand
15	Ifuho 2	7.6844	5.1827	3	1959.4	–	69.8	Gravelly sand
16	Ibong Ikot Akan	7.6775	5.1866	3	434.5	–	55.4	Fine sand
17	Ibong Road	7.6792	5.1908	3	375.5	47.5	16.0	Fine sand
18	Umuahia Road	7.6992	5.2024	3	1264.5	59.9	10.5	Coarse sand
19	Ikono Road	7.7117	5.1981	3	1506.3	–	85.4	Coarse sand
20	Progress Road	7.7069	5.1794	3	1196.1	75.7	9.0	Coarse sand

**Fig. 4** Distribution of depth to water table (a) and depth rating (b) in the study area

sands are very pervious and thus, any underlying hydrogeological units are more susceptible to contamination. Like the aquifer media, soil media were obtained from the borehole

lithologically constrained VES data interpretation results. The soil media comprise mostly sands (fine and coarse sands) and pockets of sandy clay at some locations. This

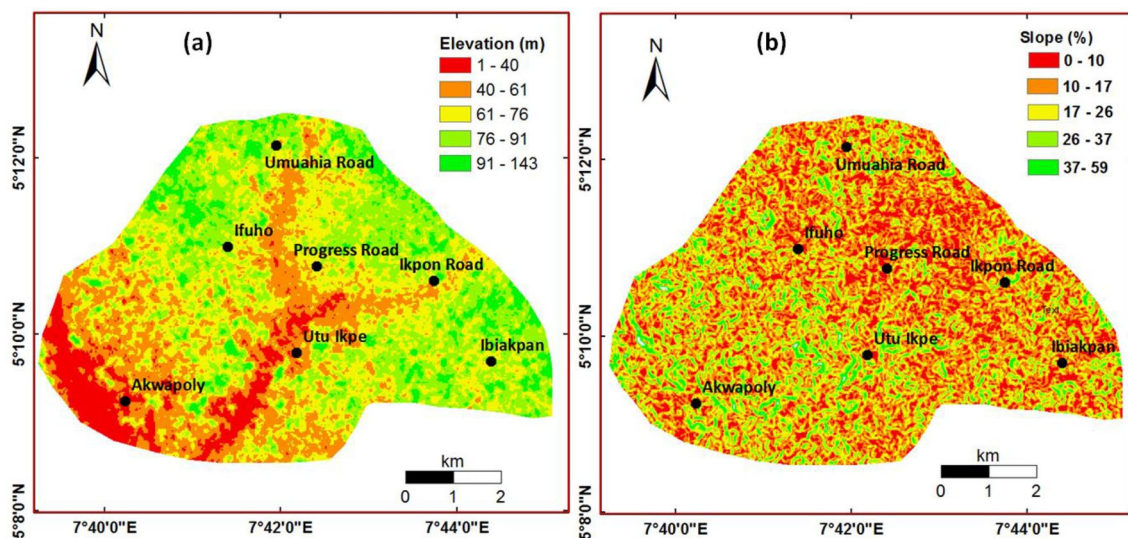


Fig. 5 Topography of the study area **a** ASTER digital elevation model (DEM), **b** slope (%) in the study area

Table 5 Net Recharge ratings for the study (Piscopo, 2001; Al-Adamat et al. 2003)

Slope (%)	Rating	Rainfall (mm)	Rating	Soil permeability	Rating	Net recharge (weight $W=4$)	Rating
<2	4	<500	1	Very slow	1	11–13	10
2–10	3	500–700	2	Slow	2	9–11	8
10–33	2	700–850	3	Moderate	3	7–9	5
>33	1	>850	4	Mod–high	4	5–7	3
				High	5	3–5	1

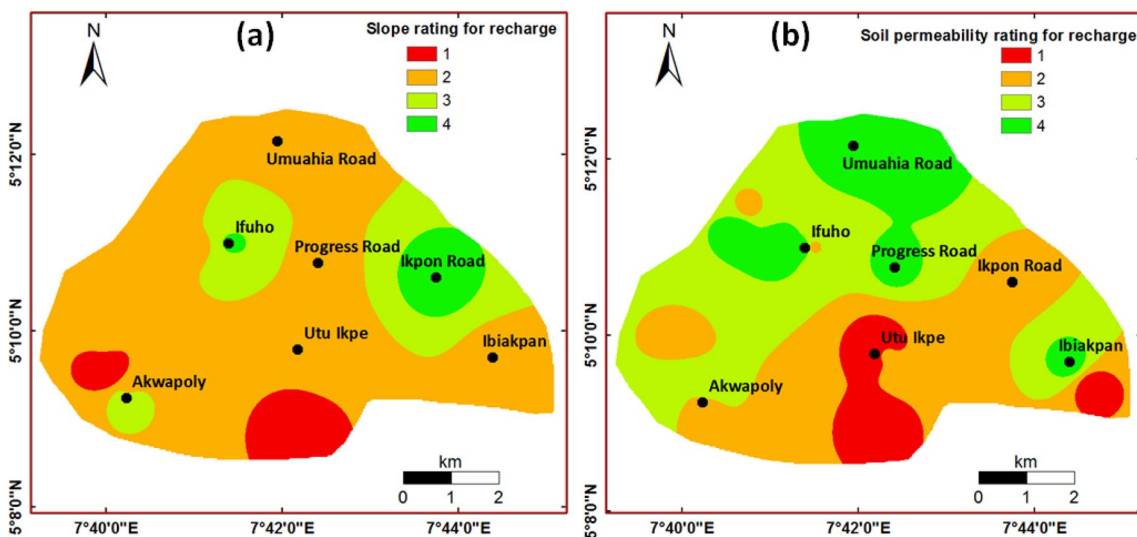


Fig. 6 Net recharge estimation: **a** slope rating, **b** soil permeability rating

parameter was thus assigned ratings of 3 for the sandy clay soil and 9 for the fine/coarse sands according to Table 1. Figure 9b shows the soil media index in the study area, which

varies between 6 and 18. About 70% of the study area is characterised by high soil media index of greater than 9

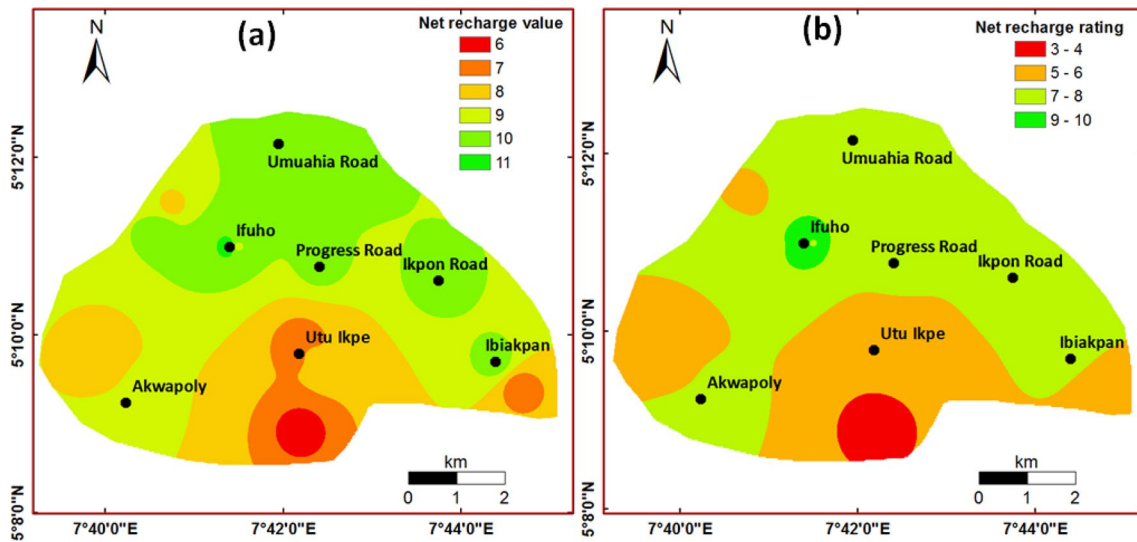


Fig. 7 Distribution of net recharge: **a** values, **b** ratings in the study area

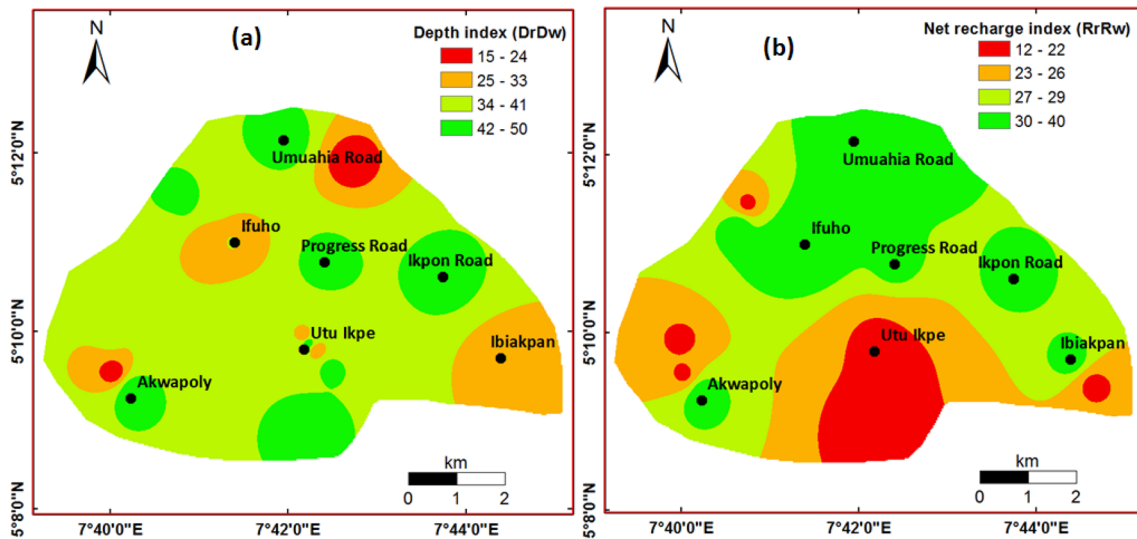


Fig. 8 Image maps of **a** Depth index, **b** net recharge index in the study area

with pockets of low index (6–9) scattered around the area as shown in Fig. 9b.

Topography this refers to the slope of the earth (land) surface. Runoff water (rainwater) will remain or flow very slowly in areas with low slope, thus allowing the percolation of contaminants to the water table. Consequently, areas with lower slopes tend to be more susceptible to contamination depending on the nature of the soil media. The slope (in %) in the study area was obtained from the ASTER digital elevation model (DEM) by the use of ArcGIS 10.5 and was assigned ratings from 1 to 10 based on Table 1. Figure 10a shows the image map of the Topography index in the study area. Figure 10a shows that the area is characterized by high

topography index of between 4 and 10 except for a pocket of low indices in the southern part of the area. The implication of this is a slow flow rate of runoff water in majority of the study area, which will enhance easy percolation of contaminants to the water table and thus high groundwater vulnerability.

Impact of vadose zone the vadose zone is the unsaturated layer that overlies the water table. This zone is particularly crucial in the percolation of rainwater into the aquifer layer (Aller et al., 1987). The vadose zone may pose a tremendous impact on flow of contaminated fluid if it is made up of pervious or permeable materials such as sands and gravels. The geomaterials of the vadose zone in this study

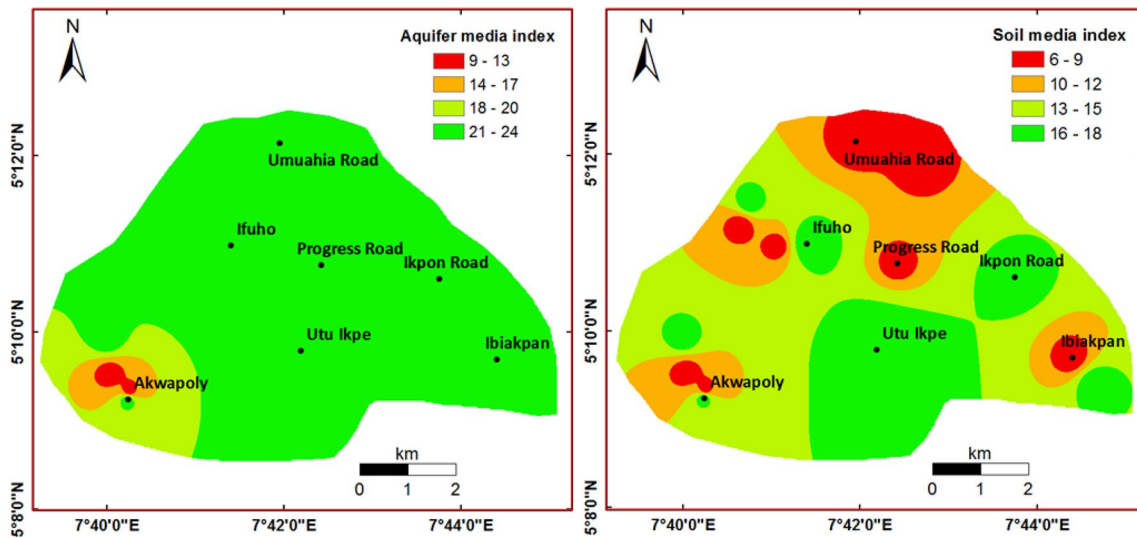


Fig. 9 Image maps of **a** Aquifer media index, **b** Soil media index in the study area

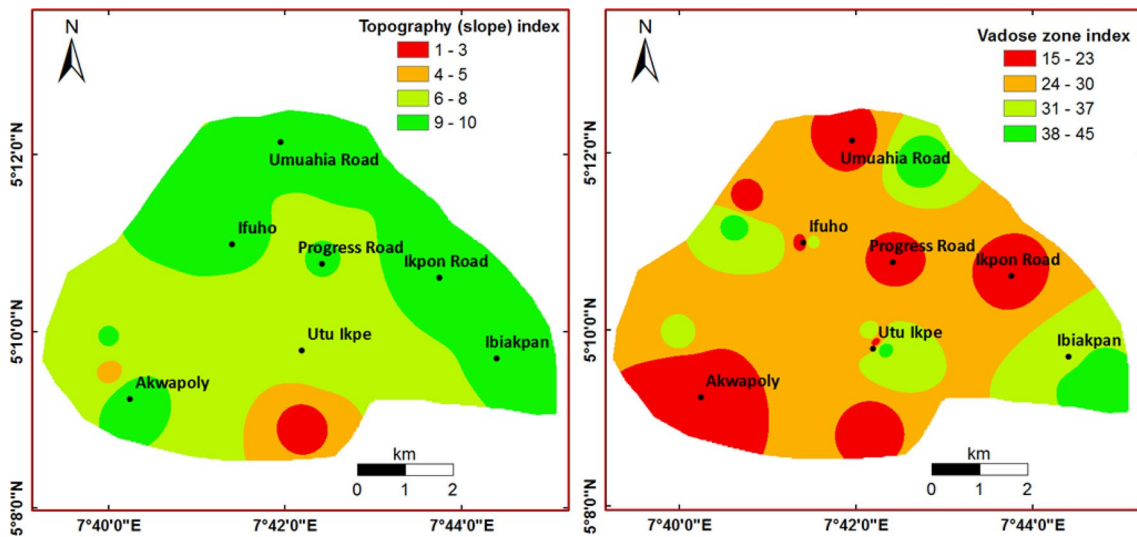


Fig. 10 Image maps of **a** Topography index, **b** Vadose zone index in the study area

were deciphered from the geological borehole lithologically constrained VES interpretation and comprise mainly sands (fine, coarse and gravelly) and sandy clay. This parameter was assigned ratings of 3 for the sandy clay, 7 for fine/coarse sands and 9 for gravelly sands according to Table 1. The weight of the parameter is 5 (Table 1). The vadose zone index in the study area ranges from 15 to 45 and is distributed as shown in the image map of Fig. 10(b), which is an indication that the study area is highly vulnerable to surface contaminants. Majority of the communities in the area is characterized by indexes of between 24 and 30 with pockets of very high indexes of between 31 and 45 and fairly low indexes of 15 to 23 distributed as illustrated in Fig. 10b. The

very high indexes correspondingly imply very high flow rate of contaminants to the water table and hence high groundwater vulnerability.

Hydraulic conductivity this is an essential property, which determines the flow rate of groundwater and hence contaminants through an aquifer. It was estimated in this study by the use Eq. (4) and ranges from 4.9×10^{-6} to 3.2×10^{-5} m/s. This range of hydraulic conductivity is consistent with the range provided by Shamsuddin et al. (2018), George et al. (2021) and George (2021) for fine to gravelly sand aquifers. The weight of this parameter is 3 and the parameter values were assigned ratings from 1 to 6 based on Table 1. The high variability of the hydraulic

conductivity is indicative of the high variability in the grain size of the geomaterial constituents of the aquifer units in the area (Ekanem, 2022; Ikpe et al., 2022). The hydraulic conductivity index in the study area varies from 3 to 18. The distribution of these indexes is shown in Fig. 11a. Low indexes of 1–7 are obtained in some locations in the north western and south western parts of the study area while the remaining parts are characterized by high indexes of 8–18. These areas with high indexes are associated with high groundwater vulnerability.

DRASTIC index (DI) and Groundwater vulnerability rating (GVR) the seven parameters discussed above were summed up according to Eq. 2 to obtain the drastic index for each of the sounding locations as summarized in Table 6. The index varies from 91 to 211 and its distribution in the study area is shown in Fig. 11b. The final groundwater vulnerability rating map was obtained from the combination of the seven DRASTIC model parameters for all the VES locations by the use of ArcGIS 10.5 (Figs. 12 and 13). The values of the DRASTIC index were reclassified based on the data in Table 2 to have three classes of vulnerability rating. These classes are respectively low (DI=91), moderate (DI=149–172) and high (DI=182–211) as shown in Fig. 12 a and b. Analysis of the GVR results shows that about 75% of the study area has high GVR while about 20% has moderate GVR and the remaining 5% has low GVR respectively (Fig. 12b). The greater percentage of moderate/high vulnerability zone in the area may be attributed to lower slope terrains in the zone coupled with the high permeable sands of the aquifer overlying layers, which facilitate rapid permeation of contaminants to the groundwater.

Sensitivity analysis of the DRASTIC model

Sensitivity analysis was carried out on the DRASTIC model results to examine the influence of the ratings and weights assigned to each of the input parameters on the final model results. This was particularly necessary because of the subjectivity in the assignment of ratings and weights to the input parameters of the model (Gogu & Dassargues, 2000b; Chit-sazan and Akhtari, 2008). The analysis was carried out by the use of two approaches. These approaches are the single parameter removal and the map removal approaches respectively. The single parameter removal approach examines the contribution of each of the input parameters to the final vulnerability index (Napolitano & Fabbri, 1996). The approach compares the theoretical assigned weights with the effective weights W (in %) computed from Eq. (6) (Napolitano & Fabbri, 1996).

$$W = \frac{(P_r \times P_w)}{V} \times 100 \quad (6)$$

where P_r is the rating value, P_w is the theoretical assigned weight and V is the unperturbed vulnerability index. The map removal sensitivity analysis on the other hand tests the influence of removing each parameter or group of parameters on the final calculated vulnerability index (Lodwick et al., 1990; Napolitano & Fabbri, 1996). The variation index (in %), which expresses the amount of variation caused by the removal of one or more parameters, was computed by the use of Eq. (7) (Napolitano & Fabbri, 1996).

$$VI_i = \frac{(V - V_i)}{V} \times 100 \quad (7)$$

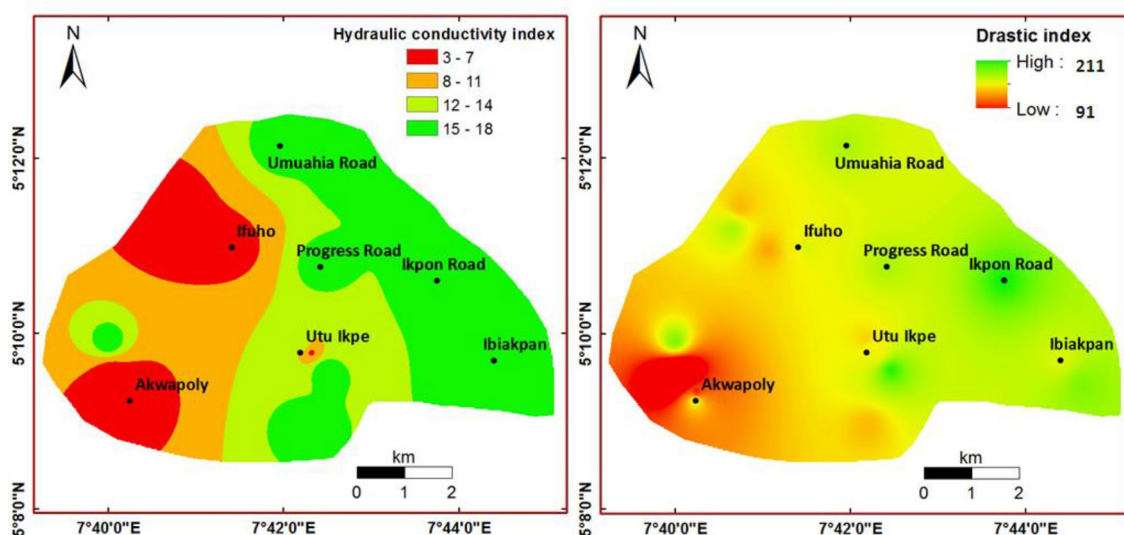


Fig. 11 Image maps of **a** Hydraulic conductivity index, **b** DRASTIC index in the study area

Table 6 Calculated DRASTIC index (DI) and groundwater vulnerability rating (GVR) in the study area

VES No	Parameter	D		R		A		S		T		I		C		DI	GVR
		Weight		4		3		2		1		5		3			
		VES Location		D_r	$D_r D_w$	R_r	$R_r R_w$	A_r	$A_r A_w$	S_r	$S_r S_w$	T_r	$T_r T_w$	I_r	$I_r I_w$		
1	Utu Ikpe 1	10	50	5	20	8	24	9	18	6	6	3	15	4	12	180	High
2	Utu Ikpe 2	5	25	5	20	8	24	9	18	6	6	7	35	4	12	179	High
3	Utu Ikpe 3	5	25	5	20	8	24	9	18	6	6	9	45	2	6	183	High
4	Utu Ikpe 4	9	45	5	20	8	24	9	18	6	6	7	35	6	18	207	High
5	Abiakpo Edem Idim	10	50	3	12	8	24	9	18	1	1	3	15	6	18	168	Moderate
6	Ibiakpan Nto Akan	5	25	8	32	8	24	3	6	8	8	7	35	6	18	188	High
7	Utu Uyo Road	5	25	5	20	8	24	9	18	8	8	9	45	6	18	203	High
8	Ikpon Road	10	50	8	32	8	24	9	18	10	10	3	15	6	18	211	High
9	Abiakpo Ntak Inyang	7	35	5	20	8	24	9	18	8	8	7	35	6	18	201	High
10	Akwa Poly P1	3	15	5	20	3	9	3	6	4	4	3	15	1	3	91	low
11	Akwa Poly P2	9	45	8	32	8	24	9	18	10	10	3	15	1	3	186	High
12	Akwa Poly P3	10	50	8	32	3	9	3	6	8	8	3	15	1	3	149	Moderate
13	Housing Ifuho	5	25	8	32	8	24	9	18	8	8	7	35	2	6	190	High
14	Ifuho 1	7	35	10	40	8	24	9	18	8	8	3	15	1	3	182	High
15	Ifuho 2	5	25	8	32	8	24	3	6	8	8	7	35	2	6	172	Moderate
16	Ibong Ikot Akan	7	35	8	32	8	24	3	6	8	8	9	45	1	3	190	High
17	Ibong Road	10	50	5	20	8	24	9	18	8	8	3	15	1	3	172	Moderate
18	Umuahia Road	10	50	8	32	8	24	3	6	8	8	3	15	6	18	189	High
19	Ikono Road	3	15	8	32	8	24	3	6	8	8	9	45	6	18	190	High
20	Progress Road	10	50	8	32	8	24	3	6	8	8	3	15	6	18	189	High

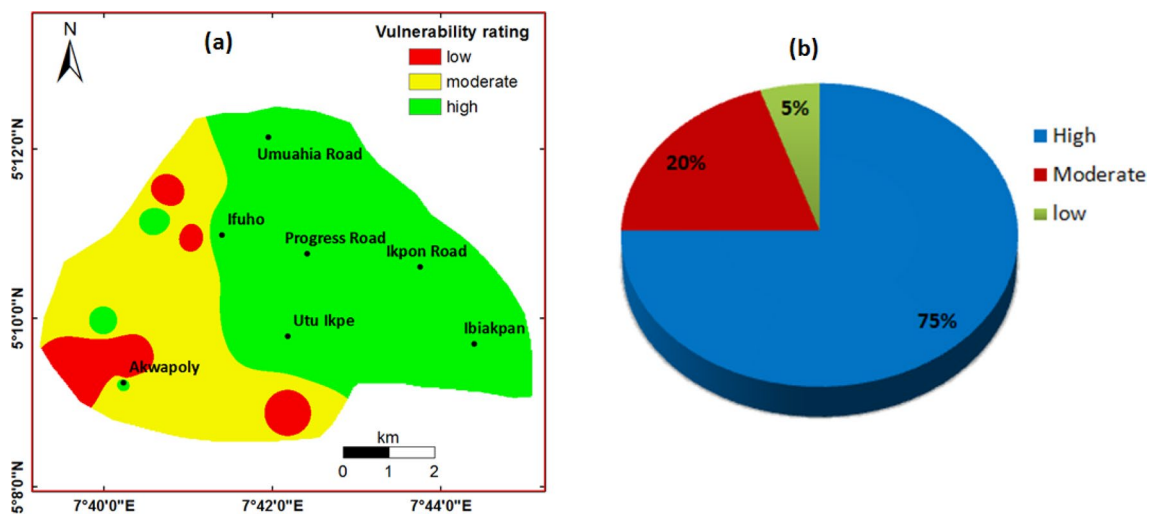


Fig. 12 Groundwater vulnerability assessment result in the study area **a** Vulnerability rating map, **b** Percentages of the three classes of vulnerability rating

where V_i is the variation index due to removal of parameter i and V_i is the perturbed vulnerability indices after the removal of parameter i . Both approaches have been successfully applied in the sensitivity analysis of DRASTIC model

(Amiri et al., 2020; Gogu & Dassargues, 2000b; Khakhar et al., 2017).

Table 7 shows the statistical summary of the DRASTIC parameters used for the computation of the final DRASTIC

Fig. 13 Bar chart showing the groundwater vulnerability ratings (GWR) of the VES stations in the study area

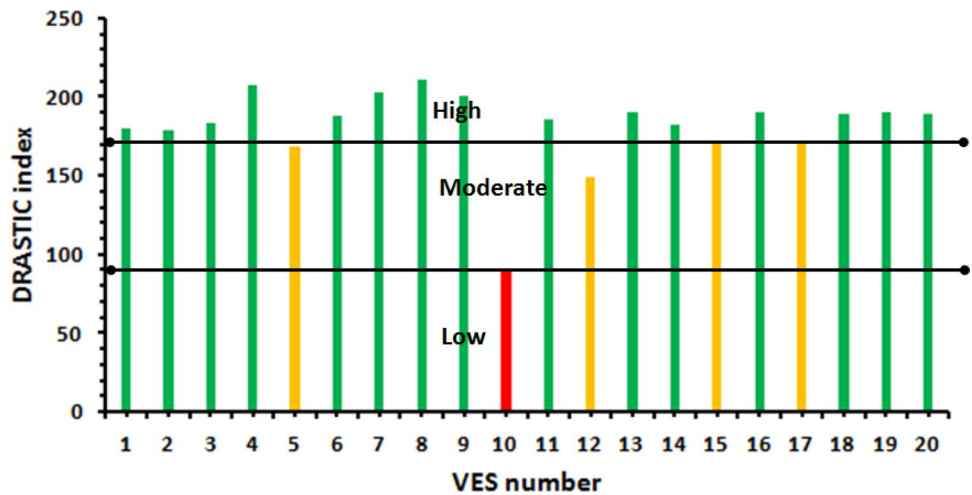


Table 7 Statistical summary of the DRASTIC parameters

	<i>D</i>	<i>R</i>	<i>A</i>	<i>S</i>	<i>T</i>	<i>I</i>	<i>C</i>
Minimum	3.0	3.0	3.0	3.0	1.0	3.0	1.0
Maximum	10.0	10.0	8.0	9.0	10.0	9.0	6.0
Mean	7.3	6.7	7.5	6.6	7.3	5.4	3.7
standard deviation	2.6	1.8	1.5	3.0	2.0	2.6	2.3
Coefficient of variation CV (%)	35.5	27.7	20.5	45.7	27.9	47.5	62.1

Table 8 Statistics of single parameter removal sensitivity analysis

Parameters removed	Mean variation index (%)
D (depth)	20.2
R (recharge)	18.7
A (aquifer media)	16.5
S (soil media)	10.9
T (topography)	8.0
I (impact of vadose zone)	17.8
C (aquifer hydraulic conductivity)	7.9

index. The mean values express the contamination risk by each of the parameters. The aquifer media poses the highest risk to groundwater contamination with a mean value of 7.5. This is followed by the depth to water table and topography (with a mean value of 7.3 each), the recharge parameter (mean value of 6.7), soil media (mean value of 6.6, impact of vadose zone (mean value 5.4) and aquifer hydraulic conductivity with a mean value of 3.7. The coefficient of variation (CV in %) expresses the contribution of each of the parameters to the overall vulnerability index variation. From Table 8, the aquifer hydraulic conductivity causes the highest variation in the vulnerability index (CV = 62.1%) while

the least variation is from the aquifer media (CV = 20.5%). Table 8 shows the results of the single parameter removal sensitivity analysis. The parameters all have variation index values of greater than unity, which implies that removing one parameter decreases the vulnerability index. The removed parameter in this case has a higher contribution to the computed vulnerability index. From Table 8, the highest variation occurs when the depth to the water table is removed (mean variation of 20.2%) followed by the net recharge (mean variation of 18.7%). A possible explanation for this is the high theoretical weights of 5 and 4 and the high ratings of 3 to 10 assigned to these parameters respectively. The variation of vulnerability is also sensitive to the removal of the vadose zone, aquifer media, soil media and aquifer hydraulic conductivity as Table 8 shows. The least variation occurs when the aquifer hydraulic conductivity parameter is removed (mean variation of 7.9%) probably due to the weight of 3 assigned to this parameter and the ratings of 1–6. Table 9 shows the vulnerability index variation caused by the removal of one or more input parameters at a time. The parameters’ removals were done in the order of increasing influence on the final vulnerability index based on the results of Table 8. The results presented in Table 9 is similar that of Table 8 with depth, net recharge and vadose zone having higher influence on the vulnerability index than the soil media, slope and aquifer hydraulic conductivity parameters.

Table 9 Statistics of map removal sensitivity analysis

Parameters used	Mean variation index (%)
DRASTI	7.9
DRASI	16.0
DRAI	28.9
DRI	43.3
DR	61.1
D	79.8

The mean values show that the vulnerability index variation increases as more input parameters are removed. This may be caused by the theoretical weights assigned to the various parameters; weaker representation of the layers compared to the site conditions and of course variations of the individual parameter within the study area (Khakhar et al., 2017). Using fewer input parameters in the DRASTIC model produces higher variations in the final vulnerability index, which is consistent with the results of Khakhar et al. (2017). This is an indication that all the DRASTIC parameters are vital in the computation of the vulnerability index. Table 10 shows the results of the single parameter sensitivity analysis. The results show that depth, net recharge, vadose zone and aquifer media constitute the most important parameters in the calculation of the final vulnerability index in this study. This also agrees with the results of the map removal sensitivity analysis.

Conclusion

The DRASTIC model and GIS techniques were employed in this study to assess groundwater vulnerability in Ikot Ekpene municipality and its environs, in southern Nigeria. Twenty vertical electrical soundings were undertaken at select locations in the study area. The result of the geological borehole lithologically constrained VES data interpretation shows that the study area is made up of 3–4 sandy layers (fine, coarse, gravels and sandy clay).

The third layer constitutes the economically exploitable hydrogeological unit in the area and occurs at a depth of 9.0–86.6 m. These findings are consistent with the results of George et al. (2014) and Ikpe et al. (2022) who used similar approach in investigating the surface characteristics in the area. Seven environmental parameters, which are depth to the water table, net recharge, aquifer media, topography, impact of vadose zone and hydraulic conductivity were used in the DRASTIC model. All the parameters, except topography were determined from the VES data interpretation results. This has the advantage of being cost effective and environmentally friendly as these parameters could be obtained swiftly from surface measurements without the need to drill any borehole (Ekanem et al., 2020; George et al., 2014, 2017, 2018; Ikpe et al., 2022; Thomas et al., 2020). Topography was determined from the ASTER digital elevation model (DEM) through the use of ArcGIS 10.5. The result of the quantile classification of the ArcGIS 10.5 shows that about 75% of the study area falls under high GVR zone, about 20% falls under moderate GVR zone while the remaining 5% falls under low GVR zone respectively. The higher percentage of the area adjudged to have moderate/high GVR may be due to the lower slope terrains in the area, which comprises mostly high permeable sandy shallow layers overlying the water table. Consequently, this part of the study area experiences easy and rapid infiltration of surface contaminants to the groundwater due to the absence of adequate impermeable protecting layers. Statistical analysis of the DRASTIC index results shows that the aquifer media poses the greatest risk to groundwater contamination, followed by depth to water table and topography. Least risk is from the aquifer hydraulic conductivity, which is shown to contribute the highest variation to the final computed DRASTIC index. The aquifer media contributes least variation to the final index. The results of the single parameter removal and the map removal sensitivity analysis indicate that final DRASTIC index is sensitive to all the parameters with the depth, net recharge, vadose zone and aquifer media constituting most important parameters. Areas with high DRASTIC index correspond to high vulnerability potential

Table 10 Statistics of single parameter sensitivity analysis

Parameter	Theoretical weight	Theoretical weight (%)	Effective weight (%)			
			Mean	Minimum	Maximum	sd
D	5	21.7	25.3	8.3	48.1	11.1
R	4	17.4	18.2	9.8	30.8	5.7
A	3	13.0	15.0	8.7	19.5	2.5
S	2	8.7	8.9	3.3	14.6	3.9
T	1	4.3	4.9	0.8	7.7	1.4
I	5	21.7	17.6	9.0	28.1	6.5
C	3	13.0	7.2	1.9	14.6	4.3

and the aquifers in these areas are poorly/weakly protected against surface or near surface contaminants.

The high groundwater vulnerability zones, which constitute 75% of the study area, have been demarcated in the vulnerability rating map generated. The demarcated zones strikingly coincide with the zones identified as having poor/weak aquifer protection by Ikpe et al. (2022). The aquifers in these demarcated zones suffer inadequate protection from surface or near surface contaminants. Consequently, the water quality from boreholes drilled in these zones may not be guaranteed and this poses great risk to human health and ecological services in the area. The vulnerability rating map no doubt provides information that may help managers, local government planners and supervisory administrations such as the Akwa Ibom State water corporation in deciding where to site boreholes in the area. The Akwa Ibom state environmental agency should ensure the construction of proper drainage and sewer systems in the study area for proper waste disposal possibly into the ravine area, where there are not residences and water boreholes. A comprehensive waste management plan should be instituted for the inhabitants of the area to follow on daily waste disposal to safeguard the already contaminant-prone aquifers in the area. A 'no dumping of solid waste policy along the road/street' should be enforced by appropriate authorities in the area. Although the groundwater vulnerability map can be used as a primary tool in identifying zones that are highly vulnerable to contamination, it cannot substitute the site-level hydrogeological investigations. Further studies involving hydrogeochemical and microbiological analyses of groundwater samples collected from available boreholes in the area to ascertain the groundwater quality are recommended to firm up the findings of this study.

Acknowledgments The authors wish to thank all who assisted in conducting this work.

Data availability The datasets generated and analysed during the current study are available from the corresponding author on reasonable request.

Declarations

Conflict of interest The author declares that there are no conflicts of interest.

References

- Abdullahi, U. (2009). Evaluation of models for assessing groundwater vulnerability to pollution in Nigeria. *Bayero Journal of Pure Applied Science*, 2, 138–142.
- Abu-Bakr, H. A. (2020). Groundwater vulnerability assessment in different types of aquifers. *Agricultural Water Management*, 240(2020), 106275. <https://doi.org/10.1016/j.agwat.2020.106275>
- Aller L, Bennett T, Lehr JH, Petty RJ, Hackett G (1987) DRASTIC: a standardised system for evaluating groundwater pollution potential using hydrogeologic settings. US-EPA Report 600/2-87-035
- Amiri, F., Tabatabaie, T., & Entezari, M. (2020). GIS-based DRASTIC and modified DRASTIC techniques for assessing groundwater vulnerability to pollution in Torghabeh-Shandiz of Khorasan County Iran. *Arabian Journal of Geoscience*, 13, 479. <https://doi.org/10.1007/s12517-020-05445-0>
- Awawdeh, M. M., & Jaradat, R. A. (2010). Evaluation of aquifers vulnerability to contamination in the Yarmouk River basin, Jordan, based on DRASTIC method. *Arabian Journal of Geoscience*, 3(3), 273–282.
- Awawdeh, M., Obeidat, M., & Zaiter, G. (2015). Groundwater vulnerability assessment in the vicinity of Ramtha wastewater treatment plant, North Jordan. *Applied Water Science*, 5, 321–334. <https://doi.org/10.1007/s13201-014-0194-6>
- Barbulescu, A. (2020). Assessing groundwater vulnerability: DRASTIC and DRASTIC-like methods: A review. *Water*, 12, 1356. <https://doi.org/10.3390/w12051356>
- Barres-Lallemend A (1994) Normalization des criteres d'etablissement desrtes de ulnerabilite aux pollutions. Etude documentaire preliminaire. BRGM R3792
- Bello, A. M. A., Makinde, V., & Coker, J. O. (2010). Geostatistical analyses of accuracies of geologic sections derived from interpreted vertical electrical soundings (VES) data: an examination based on VES and Borehole Data Collected from the Northern Part of Kwara State, Nigeria. *Journal of American Science*, 6(2), 24–31. (ISSN: 1545–1003).
- Boufekane, A., & Saighi, O. (2013). Assessment of groundwater pollution by nitrates using intrinsic vulnerability methods: A case study of the Nile valley groundwater (Jijel, North-East Algeria). *African Journal of Environmental Science Technology*, 7(10), 949–960. <https://doi.org/10.5897/AJEST2013.142>
- Chakravarthi, V., Shankar, G. B. K., Muralidharan, D., Hari-narayana, T., & Sundararajan, N. (2007). An integrated geophysical approach for imaging sub-basalt sedimentary basins: Case study of Jam River basin, India. *Geophysics*, 72(6), B141–B147.
- Civita M (1990) La valutazione della vulnerabilita degli aquifer all'inquinamento. In: Proceedings of 1st con. naz. protezione e gestione delle aque sotterranee: metodologie, tecnologie e obiettivi, 20–22 September, Maranosul Panaro, pp. 39–86
- Dobrin, M. B., & Savit, C. H. (1988). *Introduction to geophysical prospecting* (4th ed.). McGraw-Hill Book Company.
- Doerfliger, N., Jeannin, P. Y., & Zwahlen, F. (1999). Water vulnerability assessment in karst environments: A new method of defining protection areas using a multi-attribute approach and GIS tools (EPIK method). *Environmental Geology*, 39, 165–176.
- Edet, A. E., & Okereke, C. S. (2002). Delineation of shallow groundwater aquifers in the coastal plain sands of Calabar area (Southern Nigeria) using surface resistivity and hydrogeological data. *Journal of African Earth Sciences*, 35(3), 433–443.
- Ekanem KR, George NJ, Ekanem AM (2022) Parametric characterization, protectivity and potentiality of shallow hydrogeological units of a medium-sized housing estate, Shelter Afrique, Akwa Ibom State, Southern Nigeria. *Acta Geophysica*
- Ekanem, A. M. (2020). Georesistivity modelling and appraisal of soil water retention capacity in Akwa Ibom State University main campus and its environs Southern Nigeria. *Modeling Earth System and Environment*, 6, 2597–2608. <https://doi.org/10.1007/s40808-020-00850-6>
- Ekanem, A. M. (2021). Estimation of aquifer geohydrodynamic properties using the Inverse Slope method. *Researchers Journal of Science and Technology (REJOST)*, 1, 1–16.
- Ekanem, A. M. (2022). AVI- and GOD-based vulnerability assessment of aquifer units: A case study of parts of Akwa Ibom State,

- Southern Niger Delta, Nigeria. *Sustainable Water Resource Management*, 8, 29. <https://doi.org/10.1007/s40899-022-00628-x>
- Ekanem, A. M., Akpan, A. E., George, N. J., & Thomas, J. E. (2021). Appraisal of protectivity and corrosivity of surficial hydrogeological units via geo-sounding measurements. *Environmental Monitoring and Assessment*, 193, 718. <https://doi.org/10.1007/s10661-021-09518-9>
- Ekanem, A. M., George, N. J., Thomas, J. E., & Nathaniel, E. U. (2020). Empirical Relations Between Aquifer Geohydraulic-Geoelectric Properties Derived from Surficial Resistivity Measurements in Parts of Akwa Ibom State, Southern Nigeria. *Natural Resources Research*, 29(4), 2635–2646. <https://doi.org/10.1007/s11053-019-09606-1>
- Esu, E. O., Okereke, C. S., & Edet, A. E. (1999). A regional hydrostratigraphic study of Akwa Ibom State southeastern Nigeria. *Global Journal of Pure and Applied Sciences*, 5(1), 89–96.
- Fetter, C. W. (1994). *Applied hydrogeology* (3rd ed., p. 600). Prentice Hall Inc.
- Foster SSD (1987) Fundamental concepts in aquifer vulnerability, pollution risk and protection strategy. In: Duijvenbooden W, Waegeningh HG (eds) vulnerability of soil and groundwater to pollutants. TNO Committee on Hydrological Research, The Hague, Proc Info 38, 69–86
- Foster, S., Hirata, R., & Andreo, B. (2013). The aquifer pollution vulnerability concept: Aid or impediment in promoting groundwater protection? *Hydrogeology Journal*, 21(7), 1389–1392.
- George, N. J. (2021). Geo-electrically and hydrogeologically derived vulnerability assessments of aquifer resources in the hinterland of parts of Akwa Ibom State, Nigeria. *Solid Earth Sciences*, 6(2), 70–79.
- George, N. J., Akpan, A. E., & Ekanem, A. M. (2016a). Assessment of textural variational pattern and electrical conduction of economic and accessible Quaternary hydrolithofacies via geoelectric and laboratory methods in SE Nigeria: A case study of select locations in Akwa Ibom State. *Journal of the Geological Society of India*, 88, 517–528. <https://doi.org/10.1007/s12594-016-0514-6>
- George, N. J., Bassey, N. E., Ekanem, A. M., & Thomas, J. E. (2020). Effects of anisotropic changes on the conductivity of sedimentary aquifers, southeastern Niger Delta, Nigeria. *Acta Geophysica.*, 68, 1833–1843. <https://doi.org/10.1007/s11600-020-00502-4>
- George, N. J., Ekanem, A. M., Ibanga, J. I., & Udosen, N. I. (2017). Hydrodynamic Implications of Aquifer Quality Index (AQI) and Flow Zone Indicator (FZI) in groundwater abstraction: A case study of coastal hydro-lithofacies in South-eastern Nigeria. *Journal of Coastal Conservation*, 21, 759–776. <https://doi.org/10.1007/s11852-017-0535-3>
- George, N. J., Ekanem, A. M., Thomas, J. E., & Harry, T. A. (2021). Modelling the effect of geo-matrix conduction on the bulk and pore water resistivity in hydrogeological sedimentary beddings. *Modeling Earth Systems and Environment*, 8, 1335–1349. <https://doi.org/10.1007/s40808-021-01161-0>
- George, N. J., Ibuot, J. C., Ekanem, A. M., & George, A. M. (2018). Estimating the indices of inter-transmissibility magnitude of active surficial hydrogeologic units in Itu, Akwa Ibom State, southern Nigeria. *Arabian Journal of Geosciences*, 11, 134. <https://doi.org/10.1007/s12517-018-3475-9>
- George, N. J., Obiora, D. N., Ekanem, A. M., & Akpan, A. E. (2016b). Approximate relationship between frequency-dependent skin depth resolved from geoelectromagnetic pedotransfer function and depth of investigation resolved from geoelectrical measurements: A case study of coastal formation, southern Nigeria. *Journal of Earth System Science*, 125, 1379–1390. <https://doi.org/10.1007/s12040-016-0744-4>
- George, N. J., Ubom, A. I., & Ibanga, J. I. (2014). Integrated approach to investigate the effect of leachate on groundwater around the Ikot Ekpena Dumpsite in Akwa Ibom State, Southeastern Nigeria. *International Journal of Geophysics*, 174589, 1–12. <https://doi.org/10.1155/2014/174589>
- Gogu, R. C., & Dassargues, A. (2000a). Current trends and future challenges in groundwater vulnerability assessment using overlay and index methods. *Environmental Geology*, 39, 549–559.
- Gogu, R. C., & Dassargues, A. (2000b). Sensitivity analysis for the EPIK method of vulnerability assessment in a small karstic aquifer, southern Belgium. *Hydrogeology Journal*, 8, 337–345.
- Harter T, Walker LG (2001) Assessing Vulnerability of Groundwater. pp. 9–17. 35. www.dhs.ca.gov/ps/ddwem/dwsap/DWSAPindex.htm
- Ikpe, E. O., Ekanem, A. M., & George, N. J. (2022). Modelling and assessing the protectivity of hydrogeological units using primary and secondary geoelectric indices: A case study of Ikot Ekpena Urban and its environs, southern Nigeria. *Modeling Earth System and Environment*. <https://doi.org/10.1007/s40808-022-01366-x>
- Isaiah, A. I., Yamusa, A. M., & Odunze, A. C. (2021). Advanced Study on Variability in Length of Rainy Season for Selected Crops Production in Coastal and Upland Areas of Akwa Ibom State, Nigeria. *Cutting- Edge Research in Agricultural Sciences*, 6(5), 101–109. <https://doi.org/10.9734/bpi/cras/v6/2424E>
- Jaseela, C., Prabhakar, K., Sadasivan, P., & Harikumar, H. P. (2016). Application of GIS and DRASTIC modeling for evaluation of groundwater vulnerability near a solid waste disposal site. *International Journal of Geosciences*, 7, 558–571. <https://doi.org/10.4236/ijg.2016.74043>
- Khakhar, M., Ruparelia, J. P., & Vyas, A. (2017). Assessing groundwater vulnerability using GIS-based DRASTIC model for Ahmedabad district, India. *Environmental Earth Science*, 76, 440. <https://doi.org/10.1007/s12665-017-6761-z>
- Knox, R., Sabatini, D., & Canter, L. (1993). *Subsurface transport and fate processes*. Lewis Publishers.
- Kumar, A., & Krishna, A. P. (2020). Groundwater vulnerability and contamination risk assessment using GIS-based modified DRAS-TIC-LU model in hard rock aquifer system in India. *Geocarto International*, 35(11), 1149–1178. <https://doi.org/10.1080/10106049.2018.1557259>
- Li, P., Karunanidhi, D., Subramani, T., & Srinivasamoorthy, K. (2021). Sources and consequences of groundwater contamination. *Archives of Environmental Contamination and Toxicology*, 80, 1–10. <https://doi.org/10.1007/s00244-020-00805-z>
- Lodwick, W. A., Monson, W., & Svoboda, L. (1990). Attribute error and sensitivity analysis of map operations in geographical information systems: suitability analysis. *International Journal of Geographical Information System*, 4(4), 413–428.
- Machiwal, D., Jha, M. K., Singh, V. P., & Mohan, C. (2018). Assessment and mapping of groundwater vulnerability to pollution: Current status and challenges. *Earth-Science Reviews*, 185, 901–927.
- Maxe, L., & Johansson, P.-O. (1998). Assessing groundwater vulnerability using travel time and specific surface area as indicators. *Hydrogeology Journal*, 6, 441–449.
- Mbipom, E. W., Okwueze, E. E., & Onwuegbeche, A. A. A. (1996). Estimation of transmissivity using VES data from Mbaise area of Nigeria. *Nigerian Journal of Physics*, 85, 28–32.
- Napolitano, P., & Fabbri, A. G. (1996). Single-parameter sensitivity analysis for aquifer vulnerability assessment using DRASTIC and SINTACS. HydroGIS 96 Application of Geographic Information Systems in Hydrology and Water Resources Management. *IAHS*, 235, 559–566.
- Neh, A. V., Ako, A. A., Ayuk, A. R., & Hosono, T. (2015). DRAS-TIC - GIS model for assessing vulnerability to pollution of the phreatic aquiferous formations in Douala-Cameroon. *Journal of*

- African Earth Sciences*, 102, 180–190. <https://doi.org/10.1016/j.jafrearsci.2014.11.001>
- NRC (National Research Council). (1993). *Ground Water Vulnerability Assessment: Contamination Potential under Conditions of Uncertainty*. National Academy Press.
- Obaje, NG (2009) *Geology and Mineral Resources of Nigeria*. London: Springer Dordrecht Heidelberg, Pp5–14.
- Piscopo G (2001) Groundwater vulnerability map, explanatory notes, Castlereagh Catchment. Australia NSW Department of Land and Water Conservation, Parramatta. https://www.industry.nsw.gov.au/_data/assets/pdf_file/0004/151762/Castlereagh-map-notes.pdf. Accessed March 14th 2022.
- Reijers, T. J. A., & Petters, S. W. (1987). Depositional environments and diagenesis of Albian Carbonates on the Calabar Flank, SE Nigeria. *Journal of Petroleum Geology*, 10(3), 283–294.
- Shamsuddin, M. K. N., Sulaiman, W. N. A., Ramli, M. F., & Kusin, F. M. (2018). Vertical hydraulic conductivity of riverbank and hyporheic zone sediment at Muda River riverbank filtration site, Malaysia. *Applied Water Science*. <https://doi.org/10.1007/s13201-018-0880-x>
- Shirazi, S. M., Imran, H. M., Akib, S., Yusop, Z., & Harun, Z. B. (2013). Groundwater vulnerability assessment in the Melaka State of Malaysia using DRASTIC and GIS techniques. *Environment and Earth Science*, 70, 2293–2304. <https://doi.org/10.1007/s12665-013-2360-9>
- Short, K. C., & Stauble, A. J. (1967). Outline Geology of the Niger Delta. *AAPG Bulletin*, 51, 761–779.
- Stacher, P. (1995). Present Understanding of the Niger Delta hydrocarbon habitat. In M. N. Oti & G. Postma (Eds.), *Geology of Deltas: Rotterdam* (pp. 257–267). Balkema.
- Thomas, J. E., George, N. J., Ekanem, A. M., & Nsikak, E. E. (2020). Electrostratigraphy and hydrogeochemistry of hyporheic zone and water-bearing caches in the littoral shorefront of Akwa Ibom State University, Southern Nigeria. *Environmental Monitoring and Assessment*, 192, 505. <https://doi.org/10.1007/s10661-020-08436-6>
- Udoh, F. E., Nyakno, J. G., & Ekanem, A. M. (2015). Analysis of microstructural properties of Paleozoic aquifer in the Benin Formation, using Grain Size Distribution Data from Water Borehole in Akwa Ibom State, Nigeria. *IOSR Journal of Applied Geology and Geophysics*, 3(4), 25–30. <https://doi.org/10.9790/0990-03422530>
- Umoh, S. D., & Etim, E. E. (2013). Determination Of Heavy Metal Contents From Dumpsites Within Ikot Ekpene, Akwa Ibom State, Nigeria Using Atomic Absorption Spectrophotometer. *The International Journal of Engineering and Science (IJES)*, 2(2), 123–129.
- United States Environmental Protection Agency (US EPA) (1994) Handbook: Groundwater and Wellhead Protection. US EPA Report No. EPA/625/R-94/001, Washington, DC, p 239
- Van Stempvoort D, Ewert L, Was-senaar L (1992) AVI: A method for groundwater protection mapping in the prairie provinces of Canada. Prairie Provinces Water Board Report 114, Regina, SK
- Venkatesan, G., Pitchaikani, S., & Saravanan, S. (2019). Assessment of groundwater vulnerability using GIS and DRASTIC for Upper Palar River Basin, Tamil Nadu. *Journal of the Geological Society of India*, 94, 387–394. <https://doi.org/10.1007/s12594-019-1326-2>
- Vrba J, Zaporozec A (1994) Guidebook on Mapping Groundwater Vulnerability, Vol. 16. International Contribution to Hydrogeology, Hannover, 131 p.
- Vrbka, P., Ojo, O. J., & Gebhardt, H. (1999). Hydraulic characteristics of Maastrichtian sedimentary rocks of the southeastern Bida Basin, central Nigeria. *Journal of African Earth Science*, 29(4), 659–667.
- Zohdy AAR, Eaton GP, Mabey DR (1974) Application of surface geophysics to groundwater investigation. USGS techniques of water resources investigations 02-D1. <https://doi.org/10.3133/twri02D1>